Iranian Journal of Materials Forming 12 (4) (2025) 4-19

Online ISSN: 2383-0042

IJMF

Iranian Journal of Materials Forming

Journal Homepage: http://ijmf.shirazu.ac.ir

Research Article

Effect of Polymeric Additives on the Rheological Behavior of PZT Pastes for Extrusion Fiber Processing: Optimization by Taguchi Method

Sina Abedini Nia[1], Ali Shojaei Seyfabad[2] and Raziye Hayati[1*]

[1] Department of Materials Engineering, Faculty of Engineering, Yasouj University, Yasouj, Iran
[2] School of Metallurgy and Materials Engineering, Faculty of Engineering, University of Tehran, Tehran, Iran

ARTICLE INFO

Article history:

Received: 20 July 2025
Reviewed: 10 August 2025
Revised: 10 September 2025
Accepted: 13 September 2025

Keywords:

PZT fiber
Extrusion
Rheological behavior
Taguchi method
Microstructure

Please cite this article as:

Abedini Nia, S., Shojaei Seyfabad, A., & Hayati, R. (2025). Effect of polymeric additives on the rheological behavior of PZT pastes for extrusion fiber processing: optimization by Taguchi method. *Iranian Journal of Materials Forming*, *12*(4), 4-19. https://doi.org/10.22099/IJMF.2025.53739.1337

ABSTRACT

This study investigates the rheological behavior and microstructural characteristics of $Pb(Zr,Ti)O_3$ (PZT) fibers fabricated via extrusion. Using commercial soft PZT powder, polymeric additives, and an organic solvent, paste formulations were optimized through a Taguchi experimental design. The optimal composition, 5 wt.% PVB, 0.5 wt.% DBF, 0.8 wt.% SA, and 70 wt.% solid loading, achieved a viscosity of 15548 mPa·s, enabling stable extrusion. Increasing the DBF content to 2.5 wt.%, further enhanced flowability, reducing the required force and yielding a microstructure with significantly reduced surface porosity—from approximately 25% to 5.5%. After sintering at 1250 °C for 2 hours, the fibers exhibited a crack-free, homogeneous microstructure with uniformly distributed grains, as confirmed by SEM and EDAX analyses.

These findings demonstrate that precise control of paste formulation and processing parameters enables the production of high-quality PZT fibers suitable for piezoelectric applications, highlighting the industrial potential of the proposed method.

1. Introduction

Ceramic materials possess a unique combination of mechanical strength, chemical stability, and functional properties, making them indispensable in modern technologies across electronics, energy, biomedical, and aerospace sectors [1, 2]. Among these, piezoelectric ceramics are particularly valued for their ability to convert mechanical energy into electrical signals and vice versa. Lead zirconate titanate ($Pb(Zr,Ti)O_3$, PZT) remains one of the most widely used piezoelectric materials due to its high piezoelectric coefficient, thermal stability, and versatility in device integration [3-5].

* Corresponding author
E-mail address: r.hayati@yu.ac.ir (R. Hayati)
https://doi.org/10.22099/IJMF.2025.53739.1337

Recent advances have highlighted the potential of PZT fibers as a promising form factor for miniaturized and flexible piezoelectric devices. Compared to bulk ceramics, PZT fibers offer a higher surface-to-volume ratio, enhanced mechanical responsiveness, and compatibility with non-planar geometries, features that are critical for applications in wearable sensors, biomedical implants, and energy harvesting systems [6-9].

Various fabrication techniques have been explored for producing PZT fibers, including sol-gel processing, melt spinning, additive manufacturing, and extrusion. While sol-gel methods provide compositional precision, they are often limited by scalability and cost. Melt spinning enables mass production but suffers from microstructural inconsistencies [10, 11]. Among these, extrusion stands out as a cost-effective and scalable method capable of producing long, flexible fibers with controlled geometry. However, achieving optimal microstructure and piezoelectric performance via extrusion requires precise control over paste formulation and processing parameters [12, 13]. Despite extensive research, several challenges remain unaddressed. Prior studies have focused on individual parameters such as binder type or extrusion pressure, often lacking a systematic approach to paste optimization. Moreover, issues such as microstructural defects, poor homogeneity, and limited reproducibility continue to hinder the performance of extruded PZT fibers [14-18]. In our previous work, PZT fibers were successfully fabricated via extrusion using a conventional solvent system comprising PVA, glycerol, and deionized water. While that study demonstrated the feasibility of fiber formation and achieved promising microstructural results, it lacked a systematic approach to paste optimization and rheological control. Building on that foundation, the present research employs a Taguchi experimental design to investigate the influence of polymeric additives and solid loading on the rheological behavior of PZT pastes. This approach enables the formulation of an optimized paste for extrusion, aiming to produce crack-free, homogeneous fibers with enhanced structural integrity and suitability for piezoelectric applications [19].

Commercially available PZT powder was used as the solid load, and polymeric additives, namely polyvinyl butyral (PVB), dibutyl phthalate (DBF), and stearic acid (SA), were incorporated during the attrition milling process. A Taguchi L9 orthogonal array was employed to systematically evaluate the effects of additive concentrations and solid loading on the rheological properties of the paste. The optimized pastes were processed via extrusion, and the influence of each parameter on viscosity and flowability was analyzed. Subsequently, PZT fibers were fabricated and sintered under controlled thermal conditions. Unlike previous studies that lacked systematic formulation strategies or resulted in microstructural defects, this work demonstrates a reproducible method for producing crack-free, homogeneous PZT fibers with tailored rheological properties. The novelty of this research lies in the integration of statistical design with extrusion-based fabrication to achieve structurally robust fibers suitable for piezoelectric applications.

2. Materials and Methods

In this study, piezoelectric fibers were fabricated using commercially available lead zirconate titanate powder (PZT-5A) as the functional ceramic phase. Polyvinyl butyral (PVB) was employed as a binder to enhance the green body strength, while dibutyl phthalate (DBF) served as a plasticizer to improve flexibility during shaping. Stearic acid (SA) was added as a dispersing agent to promote homogeneous particle distribution, and ethanol was used as the solvent to facilitate slurry preparation. This formulation builds upon previous studies that demonstrated the effectiveness of similar compositions in achieving uniform and defect-free ceramic fibers [19-21]. The detailed specifications of the raw materials are presented in Table 1.

The Taguchi method was employed to optimize the extrusion-based fabrication of PZT fibers. By selecting an appropriate orthogonal array (OA) based on the number of variables and their respective levels, researchers can efficiently conduct experiments and identify optimal process conditions.

Table 1. Specifications of the raw materials used in this research

Material	Chemical formula	Purity (%)	Company/Country
PZT	Commercial PZT-5A	≥99	China
DBF	C_6H_4-1,2-$[CO_2(CH_2)_3CH_3]_2$	≥99	Sigma-Aldrich
PVB	$(C_8H_{14}O_2)_n$	≥99	Sigma-Aldrich
SA	$C_{18}H_{36}O_2$	≥99	Merck

The results are analyzed statistically, and signal-to-noise (S/N) ratio graphs are utilized to determine the most favorable parameter settings, as well as to assess the influence of each individual factor on the response variable [22]. Specifically, an L9 OA was used to systematically vary four key parameters in the paste formulation: the concentrations of dibutyl phthalate (DBF), stearic acid (SA), polyvinyl butyral (PVB), and solid content. Each factor was assigned three levels, as detailed in Table 2. While a full factorial design would require 81 experimental runs, the Taguchi approach reduced this number to just 9, significantly minimizing resource consumption while maintaining statistical robustness. The use of Taguchi design in ceramic processing has been shown to significantly reduce experimental workload while maximizing insight into factor interactions and process optimization [23]. The specific quantities of each component used in the nine formulations are presented in Table 3, which served as the basis for paste preparation. This structured approach enabled efficient evaluation of the influence of each variable on the rheological behavior, extrusion quality, and final microstructure of the PZT fibers.

It should be noted that this study relies solely on the Taguchi experimental design method rather than theoretical or computational modeling. While it effectively analyzes the impact of additive concentrations on rheological behavior with minimal experiments, its predictive power is limited to the tested conditions. Due to assumptions of linearity and minimal interaction effects, the method may not be suitable for highly nonlinear or complex systems. Therefore, the results should be interpreted within the boundaries of the specific experimental setup and material system.

The paste was prepared by mixing PZT-5A powder with the designated additives in an attrition mill.

Table 2. The factors and their levels studied in the PZT paste of this research

Levels	Processing variables			
	PVB (wt.%)	DBF (wt.%)	SA (wt.%)	Solid in paste (wt.%)
Level 1	5	0.5	0.8	70
Level 2	7.5	1	1.25	75
Level 3	10	1.5	1.66	80

Table 3. The data of PZT paste including the variables and the number of experiments that were conducted based on the L9 orthogonal array of Taguchi method

Sample	PVB (wt.%)	DBF (wt.%)	SA (wt.%)	Solid in paste (wt.%)
1	5	0.5	0.8	70
2	5	1	1.25	75
3	7.5	1.5	0.8	75
4	10	1	0.8	80
5	5	1.5	1.66	80
6	10	0.5	1.66	75
7	10	1.5	1.25	70
8	7.5	1.66	1	70
9	7.5	0.5	1.25	80

Specifically, PZT powder and additives were placed in polymer containers with ethanol, the amount calculated according to the desired solid loading (wt.%). The mixture was subjected to attrition milling at 250 rpm for 2 hours. During milling, the process was paused twice to scrape paste from the container walls using a spatula, ensuring uniform dispersion and preventing material buildup. This procedure yielded a homogeneous paste suitable for extrusion. To stabilize the rheological behavior, the paste was aged for 24 hours before viscosity measurement. Rheological characterization was performed using an Anton Paar rotational rheometer (Austria).

After paste preparation, fiber formation was performed via extrusion using a uniaxial pressing machine, a method widely employed in ceramic fiber fabrication for its scalability and geometric control [23, 24]. The extruded samples were dried at ambient conditions and subsequently sintered at 1250 °C, based on prior optimization studies that identified this temperature as suitable for achieving dense, crack-free PZT microstructures [19].

Following paste preparation, fiber formation was carried out via extrusion using a uniaxial pressing machine, a method widely employed in ceramic fiber fabrication due to its scalability and geometric control

[23, 24]. Uniaxial pressing also enhances the texturing and piezoelectric response of ceramic microfibers [25]. The extrusion was performed using a steel die with a 300 µm outlet diameter. Pressure was applied gradually through a piston under a manual press. Given the die size and paste consistency, the flow rate was approximately 0.5–1 mm/s, ensuring smooth shaping without structural defects. The extruded fibers were dried at 100 °C for 12 hours, followed by binder burnout and sintering at 1250 °C for 2 hours. Bulk density was measured using the Archimedes method, calculated from the weight difference according to Archimedes' principle. The particle size distribution of the initial powder was analyzed using field emission scanning electron microscope (FE-SEM, TESCAN, Czech Rep.). Micrographs processed with ImageJ software. Microstructural analysis was conducted with a VEGA3 TESCAN SEM, and elemental mapping was performed via energy-dispersive X-ray spectroscopy (EDAX) using an Oxford Instruments system. These techniques enabled detailed evaluation of grain morphology, porosity, and phase distribution, which are critical for assessing the quality and functionality of sintered PZT fibers. Surface porosity of the fiber samples was evaluated based on SEM image analysis. High-resolution SEM micrographs of raw and sintered fibers were analyzed in ImageJ. Images were converted to binary format, and thresholding distinguished pore regions from solid areas. Porosity was calculated as the percentage of black (pore) pixels relative to the total image area, providing a comparative estimate of surface porosities.

3. Results and Discussion

Fig. 1 shows the Taguchi analysis used for process optimization based on the constituent components. According to the figure, the highest mean signal-to-noise (S/N) ratios for PVB were observed at 5 wt.% and 10 wt.%. For DBF, the optimal value was found to be 0.5 wt.%, while for stearic acid, it was 0.8 wt.%. The optimal solid content was 70 wt.% and 80 wt.%. In the Taguchi method, the signal-to-noise (S/N) ratio measures system response variability caused by noise factors or external disturbances. The optimal region included combinations with 5–10 wt.% PVB, 0.5–1 wt.% DBF, 0.8 wt.% SA, and 70–80 wt.% solid loading. Because multiple S/N maxima occurred at different levels for certain factors, a single optimal value could not be assigned to each parameter. Sample 1 (5 wt.% PVB, 0.5 wt.% DBF, 0.8 wt.% SA, 70 wt.% solids) was chosen as the optimal formulation because it matched the S/N-optimal levels for all four factors, providing the most consistent and balanced rheological performance.

Variations in the S/N ratio directly affect process parameter optimization. A higher S/N ratio indicates greater robustness against noise, leading to reduced variability in the system's response. This improvement reflects enhanced process stability and reliability. Thus, a higher S/N ratio indicated lower sensitivity to external factors and better performance, a key objective of the

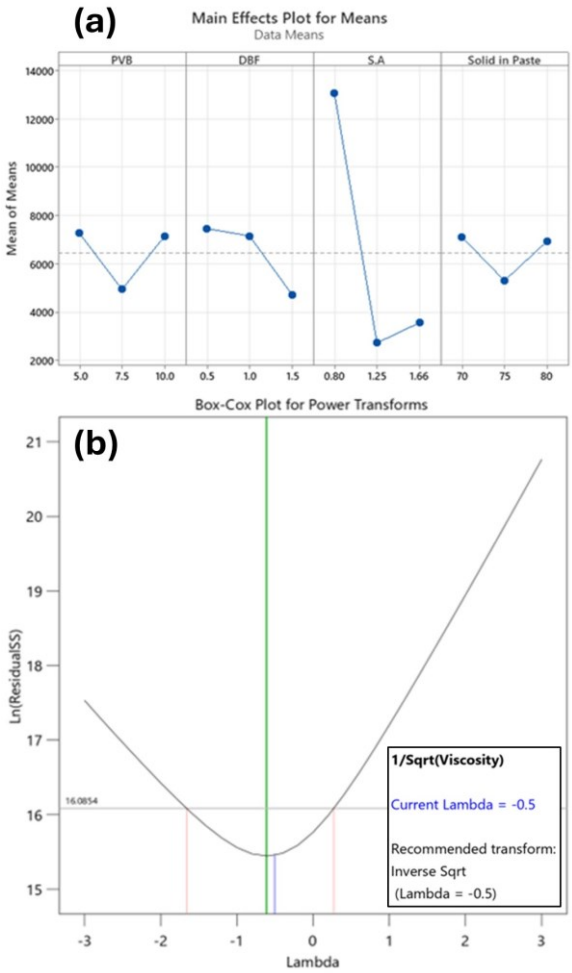

Fig. 1. Taguchi analysis of process parameter optimization based on constituent components; (a) main effects plots for means, and (b) the Box-Cox plot.

Taguchi method, which minimizes variability and improves final product quality [26, 27]. The Box-Cox plot is a statistical tool used to improve data normality and reduce variance heterogeneity. In this plot, the horizontal axis represents the lambda (λ) parameter, while the vertical axis displays the log-likelihood value or another optimization criterion, such as the signal-to-noise (S/N) ratio. The primary objective of the Box-Cox plot is to identify the optimal λ value that yields the most effective data transformation. The plot peak corresponds to the optimal λ value, indicating the transformation that should be applied to improve normality or stabilize variance.

A sharper and more pronounced peak suggests a stronger and more reliable transformation, reinforcing the effectiveness of the chosen λ in optimizing the dataset [28, 29]. Analysis of Fig. 1 reveals an optimal lambda (λ) value of -0.5, indicating that an inverse transformation is the most suitable approach for this dataset. Furthermore, based on the Taguchi experimental design, it can be concluded that samples 1-6 were processed under optimal conditions.

3.1. Investigation of additive interactions on paste viscosity

To systematically evaluate the combined effects of additive concentrations on rheological behavior, Fig. 2 presents a binary analysis of additive interactions on paste viscosity. As shown in Fig. 2(a), when PVB content is held constant, formulations containing 0.8 wt.% stearic acid (SA) exhibit maximum viscosity values. Conversely, at fixed SA concentrations, the highest viscosity is observed in samples with 5 wt.% polyvinyl butyral (PVB). The observed viscosity increases with reduced PVB and SA concentrations can be attributed to their dual roles as plasticizers and lubricants in ceramic processing. PVB serves as both a polymeric binder and a plasticizer, enhancing particle cohesion through polymer bridging, improving paste flow characteristics via network formation, and reducing interparticle friction through lubrication effects. The viscosity modulation mechanism therefore operates through polymer network formation that maintains particle dispersion, flow enhancement by lowering internal friction between PZT particle dispersion, and prevention of particle agglomeration. When PVB concentrations decrease below optimal levels, the polymer network becomes insufficient to maintain particle separation, and the resulting paste exhibits significantly higher viscosity. This analysis underscores the critical balance between binder content and lubrication effects required to achieve optimal paste rheology for ceramic processing applications [30].

Stearic acid also functions as a lubricant in PZT manufacturing, reducing interparticle friction by forming a protective coating on powder surfaces. This action enhances the flowability of the ceramic paste, facilitating smoother processing. However, when SA content decreases, friction between particles intensifies, promoting aggregation and stiffening of the paste. Consequently, diminished flowability and increased resistance to deformation lead to higher viscosity [31]. From a colloidal stability perspective, stearic acid adsorbs onto PZT particle surfaces via its polar head group, forming a steric barrier that prevents close particle approach. This mechanism aligns with DLVO theory, where steric and electrostatic repulsion counteract van der Waals attraction, thereby enhancing dispersion and reducing agglomeration [32]. A simultaneous reduction in both PVB and SA amplifies their individual effects, leading to a significant increase in paste viscosity.

As illustrated in Fig. 2(b), reducing the amount of DBF leads to an increase in viscosity. This reduction significantly influences the rheological behavior of the PZT ceramic paste. DBF, a liquid plasticizer, functions as a softener and lubricant, mitigating interparticle friction through surface adsorption and enhancing paste flowability. By reducing internal resistance, DBF lowers viscosity, facilitating easier shaping and extrusion [33].

Fig. 2(c) confirms that solid content governs paste viscosity by modulating the balance between particulate solids and the liquid phase. Elevated solid loading increases viscosity through three key effects: (1) reduced interparticle distance, which strengthens van der Waals and electrostatic forces, enhancing particle aggregation

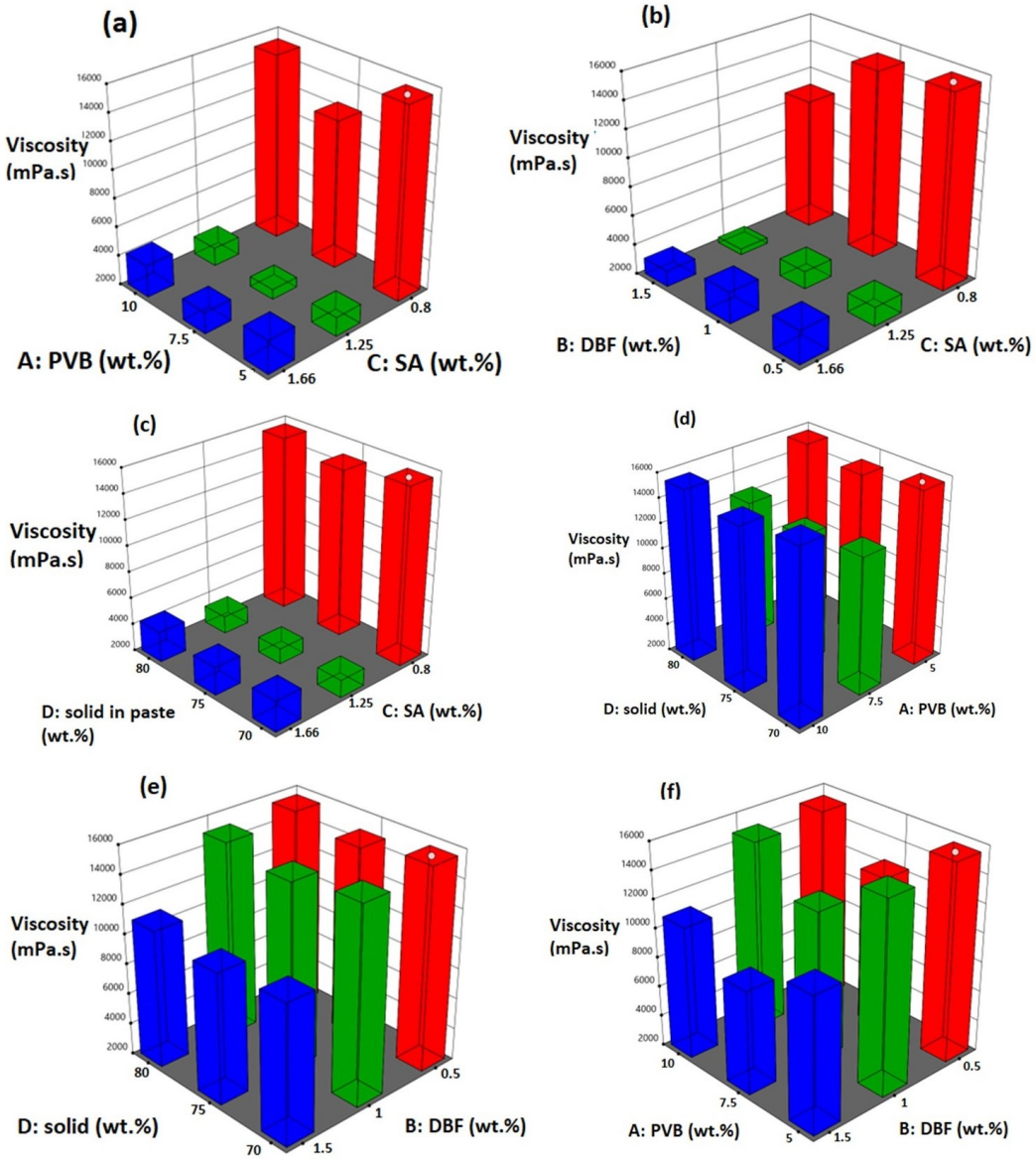

Fig. 2. Diagrams of binary effects of process parameters obtained from DOE software: (a) PVB versus SA, (b) DBF versus SA, (c) Solid content in paste versus SA, (d) Solid content versus PVB, (e) Solid content versus DBF, and (f) PVB versus DBF.

and flow resistance; (2) decreased liquid-phase availability which limits particle lubrication and increases friction; and (3) potential network formation at high concentrations, where particles interconnect to restrict deformation and amplify viscous response [34]. The increase in viscosity follows a nonlinear relationship with solid loading, which can quantitatively be described by modified Krieger-Dougherty or Mooney equations for concentrated suspensions [35, 36].

Fig. 2(d), demonstrates the simultaneous effect of solid load and PVB concentrations in the paste. The results show that solid fraction and binder content do not act independently, but cooperatively or competitively determine viscosity through mechanisms of particle packing, friction, and lubrication. The non-monotonic trend (70% → 75% dip → 80% peak) reveals a packing efficiency window at 75% solids, while the inverse relationship between binder and viscosity at 70% solids highlights that additional binder is not always beneficial. This analysis provides critical insights into the rheological behavior of ceramic pastes, emphasizing the interplay between formulation parameters and flow characteristics. It further suggests a roadmap for formulating: (1) target 75% solids for the best extrudability, (2) use moderate-to-high binder (7.5-10% PVB) at 75% solids, (3) Avoid 10% PVB at 70% solids,

it backfires, and (4) 80% solids is likely too ambitious without advanced processing aids.

Another set of interactions is illustrated in Fig. 2(e), combining solid load fraction with DBF content. Solid fraction and plasticizer concentration interact to govern viscosity through particle packing efficiency and interparticle friction [37]. The non-monotonic solid fraction trend is universal, while DBF's effect is straightforward: higher content consistently reduces viscosity by acting as a lubricant. Unlike PVB, DBF does not exhibit an over-lubrication penalty at low solids, making it a robust tool for viscosity reduction. The optimal formulation for extrudability combines the packing efficiency of 75% solids with the maximum lubrication effect of 1.5% DBF.

The last graph shows the variations of viscosity with PVB and DBF weight percentages (Fig. 2(f)). The data reveal that the viscosity of PZT pastes is strongly influenced by the synergistic interaction between PVB (binder) and DBF (plasticizer), with a non-monotonic relationship for both additives. The lowest viscosity occurs at 7.5 wt.% PVB and 1.5 wt.% DBF, where PVB provides sufficient binding without excessive thickening, and DBF optimally lubricates particle surfaces. At 5 wt.% PVB, viscosity is high due to insufficient binder, while at 10 wt.% PVB, viscosity increases again because of polymer entanglements. Similarly, 1.5 wt.% DBF consistently reduces viscosity more effectively than lower concentrations (0.5–1 wt.%), which fail to fully lubricate the system. The results indicate that 7.5 wt.% PVB combined with + 1.5 wt.% DBF is the optimal formulation for balancing low viscosity and structural integrity, while higher PVB or lower DBF concentrations result in suboptimal rheological behavior [38]. This underscores the importance of precise additive ratios to achieve processable pastes with minimal defects.

These findings are in agreement with previous studies. Wu et al. [31] reported that stearic acid reduces interparticle friction and improves flowability in PLZT ceramics via surface modification. Similarly, Nie et al. [33] demonstrated that DBF significantly lowers viscosity and facilitates shaping in ceramic pastes designed for additive manufacturing. These comparisons confirm that the rheological behavior observed in the present formulations is consistent with established mechanisms reported in the literature.

3.2. Rheological considerations in PZT fiber processing

To determine the optimal additive composition for subsequent processing, the influence of varying additive concentrations on paste rheological behavior was systematically evaluated. Fig. 3 presents the viscosity profiles as a function of shear rate, while Fig. 4 provides a comparative analysis of average viscosity values across different formulations. The rheological characterization revealed distinct viscosity trends among the samples: sample 1 exhibited the highest viscosity (15548 mPa·s), sample 4 demonstrated the second highest viscosity (14937 mPa·s), sample 3 showed intermediate viscosity values, and the remaining samples displayed significantly lower viscosities ranging between 2300-4100 mPa·s.

The formulation yielding maximum viscosity (Sample 1) was characterized by 5 wt.% polyvinyl butyral (PVB), 0.5 wt.% dibutyl phthalate (DBF), 0.8 wt.% stearic acid (SA), and 70 wt.% solid loading. This optimized composition demonstrates superior rheological properties suitable for subsequent processing requirements.

Viscosity represents a critical parameter in both the fabrication and functional performance of piezoelectric ceramics such as lead zirconate titanate (PZT). During PZT manufacturing, elevated viscosity imparts enhanced flow resistance to the material system, which proves particularly advantageous in forming operations. This increased resistance to deformation enables superior shape retention during extrusion processes, facilitating the production of components with precise dimensional control and structural integrity [39, 40].

The variations in shear stress as a function of shear strain for different PZT pastes in this study are demonstrated in Fig. 5. The fluctuations in shear stress values in samples 4 and 6, accompanied by lower viscosity values at elevated shear rates, confirm the shear thining

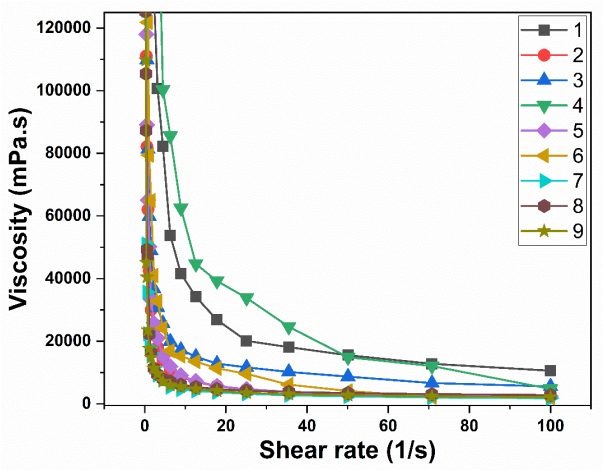

Fig. 3. Viscosity as a function of shear rate for different samples.

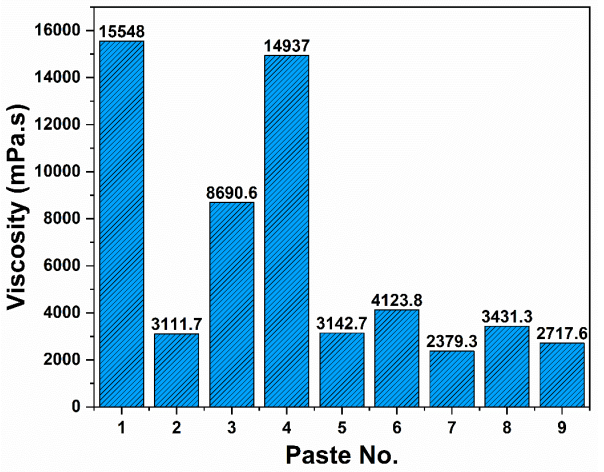

Fig. 4. Viscosity values for different PZT pastes (samples 1-9).

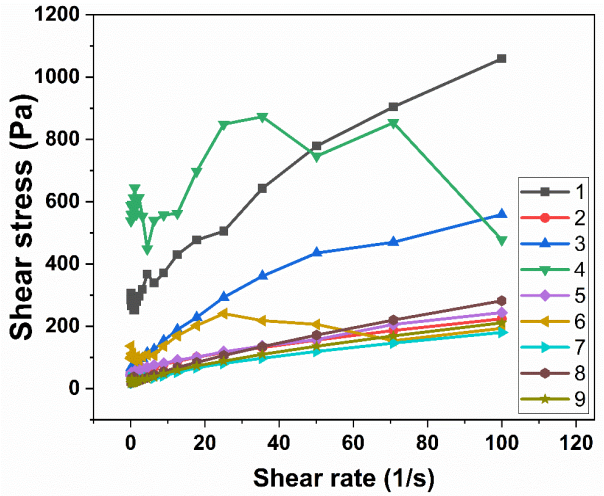

Fig. 5. The variations in shear stress versus shear strain in different PZT pastes (1-9).

behavior. Other samples showed approximately similar trends, while the non-linear increase in shear stress values of pastes 1 and 3 indicates a different rheological behavior.

The non-linear increase in shear stress versus shear rate in some pastes can be interpreted through the behavior of agglomerates and their structural changes under shear. The mechanism of breakage involves the stretching of agglomerate structures rather than compression, which contributes to the non-linear correlation observed in stress-time curves [41]. The rheological behavior of ceramic suspensions during extrusion significantly impacts the quality of the produced parts. Understanding these behaviors is crucial for optimizing the extrusion process ensuring high-quality ceramic products. By analyzing the data from Figs. 1-4, sample 1, also predicted by the Taguchi method, was selected as the optimal paste, with the following formulation: 5 wt.% PVB, 0.5 wt.% DBF, 0.8 wt.% SA, and 70 wt.% solid loading. This optimized composition demonstrates superior rheological properties suitable for subsequent processing requirements.

Previous studies on ceramic paste extrusion have primarily focused on empirical shaping outcomes, often without providing quantitative rheological analysis or predictive modeling of viscosity behavior. To address this gap, the Krieger–Dougherty equation was employed to model the viscosity of ceramic suspensions as a function of particle volume fraction [42], which relates relative viscosity (η_r) to the particle volume fraction (ϕ) as follows:

$$\eta_r = (1 - \frac{\emptyset}{\emptyset_m})^{-\eta[\phi_m]} \quad (1)$$

Where ϕ_m is the maximum packing fraction and η is the intrinsic viscosity. The observed peak in viscosity at 0.8 wt.% stearic acid corresponds to a state where interparticle repulsion is maximized, effectively increasing the hydrodynamic volume and approaching ϕ_m. Beyond this concentration, excess SA may lead to particle surface saturation or phase separation, reducing effective volume fraction and thus lowering viscosity. This trend aligns well with the theoretical prediction of the Krieger-Dougherty model.

Although the Krieger-Dougherty equation was

introduced to conceptually describe the influence of solid loading on paste viscosity, its quantitative application was not pursued due to the multifactorial nature of the experimental design. The Taguchi L9 array involved simultaneous variation of four parameters, including polymer and plasticizer content, which significantly influenced the rheological behavior. As a result, the viscosity trends did not follow a monotonic pattern with respect to solid volume fraction, and the model was used solely as a qualitative framework.

The observed peak in viscosity at 0.8 wt.% stearic acid corresponds to a state of maximized interparticle repulsion, effectively increasing the hydrodynamic volume and approaching the maximum packing fraction (ϕ_m). Beyond this concentration, excess SA may lead to particle surface saturation or phase separation, reducing effective volume fraction and thereby lowering viscosity. This behavior aligns well with the theoretical prediction of the Krieger–Dougherty model. Integrating rheological modeling with experimental extrusion data provides a predictive framework for optimizing ceramic paste formulation—an approach not previously reported in the context of PZT fiber fabrication.

Although most prior studies on PZT fiber extrusion do not report explicit viscosity values, successful fiber formation and defect-free sintering suggest that low-to-moderate viscosity ranges are preferable [13, 16, 18, 43]. Based on reported performance and comparable ceramic paste studies, an inferred optimal range of 10–30 Pa·s appears reasonable [18]. In our study, the optimized viscosity of ~15 Pa·s falls within this range and is supported by the successful fabrication of uniform, crack-free PZT fibers.

3.3. Microstructural evaluations

The morphology and particle size distribution of the PZT powder were analyzed using scanning electron microscopy (SEM) and ImageJ software. SEM micrographs (Fig. 6) revealed that the particles exhibited a predominantly irregular shape with slight agglomeration. Quantitative analysis of particle size distribution was performed on the SEM images using ImageJ, indicating an average particle size of approximately 400 nm, with a distribution range from 100 to 750 nm. These characteristics are critical for ensuring uniform dispersion and effective interaction within the paste.

Following the selection of paste 1 as the optimal formulation and its subsequent extrusion, the microstructure of the PZT sample was examined using scanning electron microscopy. Fig. 7 presents SEM micrographs at different magnifications, revealing the key morphological features. The microstructure of extruded PZT is strongly process-dependent, being influenced by extrusion parameters, drying conditions, and post-forming treatments such as sintering. As shown in the SEM images, the sample exhibits a dense microstructure with minimal porosity, indicative of effective processing. Porosity, observed as dispersed cavities of varying sizes, can significantly affect both the mechanical integrity and piezoelectric performance of

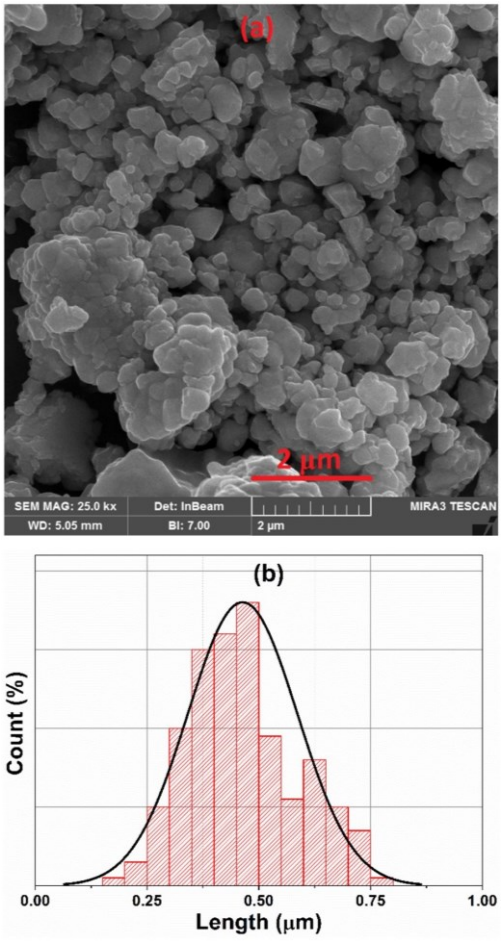

Fig. 6. (a) SEM micrographs of PZT powder, and (b) the corresponding grain size distribution obtained using ImageJ analysis.

the material. The micrographs also display polygonal PZT grains with a size distribution characteristic of ceramic extrusion. Importantly, no evidence of microcracks, fractures, or other structural defects was detected. The observed porosity is mainly attributed to air entrapment during extrusion, with additional contributions from volatilization of processing aids during thermal treatments.

Initial elemental analysis of the sample surface confirmed the presence of oxygen, carbon, lead, titanium, and zirconium, consistent with the PZT composition and the residual organic additives. To further evaluate the spatial distribution of these elements, Fig. 8 presents the elemental mapping of the fiber extruded from the optimize paste (sample 1). The mapping reveals that oxygen (O), zirconium (Zr), lead (Pb), and titanium (Ti) exhibit are uniformly distributed across the microstructure. In contrast, carbon (C) appears concentrated around pore regions, suggesting its origin from residual organic compounds or processing aids. Fig. 9 presents the SEM analysis of the extruded fiber fabricated from paste 1 with increased DBF content, revealing a notable reduction in porosity and a significant enhancement in microstructural homogeneity. The elevated DBF concentration suppresses viscosity by promoting polymer chain mobility and interparticle lubrication, thereby facilitating smoother extrusion. This rheological optimization adjustment reduces die-wall friction, lowers extrusion pressures, and alleviates internal shear stresses, critical factors in minimizing defect formation such as microcracks or warpage. This resulting microstructural uniformity translates directly into improved mechanical properties (e.g., fracture toughness) and a more consistent electromechanical response by mitigating property gradients and stress concentrations [44]. Nevertheless, excessive DBF content may introduce drawbacks, as residual organics from incomplete burnout during sintering can increase porosity and reduce final density, potentially impairing piezoelectric performance [45]. Hence, DBF concentration must be carefully optimized to balance between enhanced flowability during extrusion and the structural as well as functional integrity of the sintered fibers.

EDS analysis of the sample surface after treatment with 2.5 wt.% DBF (Fig. 9(c)) revealed that the microstructure primarily composed of lead and oxygen, trace amounts of titanium and zirconium also detected. To further clarify these results, Fig. 9(d) presents the elemental distribution maps. The mapping confirms that Ti, Zr, Pb, and O are uniformly distributed across the surface.

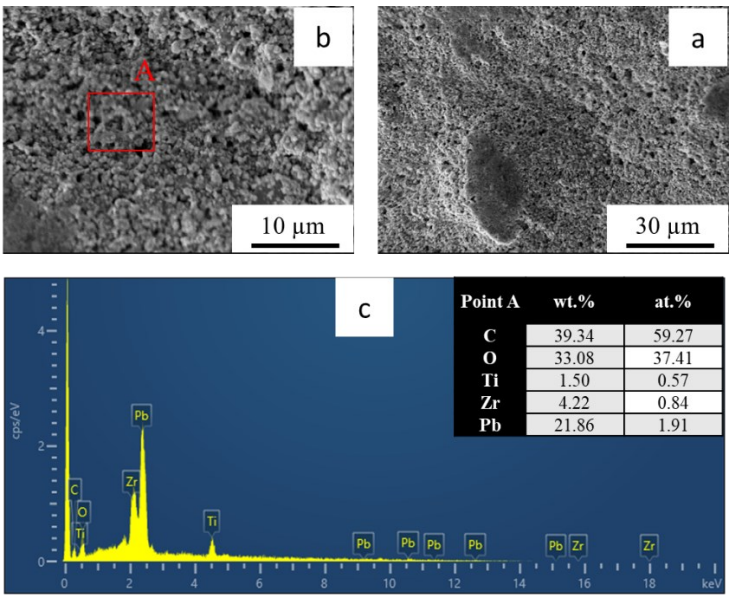

Fig. 7. SEM micrographs of the surface of the raw fiber extruded from the optimized paste at two magnifications: (a) low and (b) high, along with (c) EDS analysis of the sample surface.

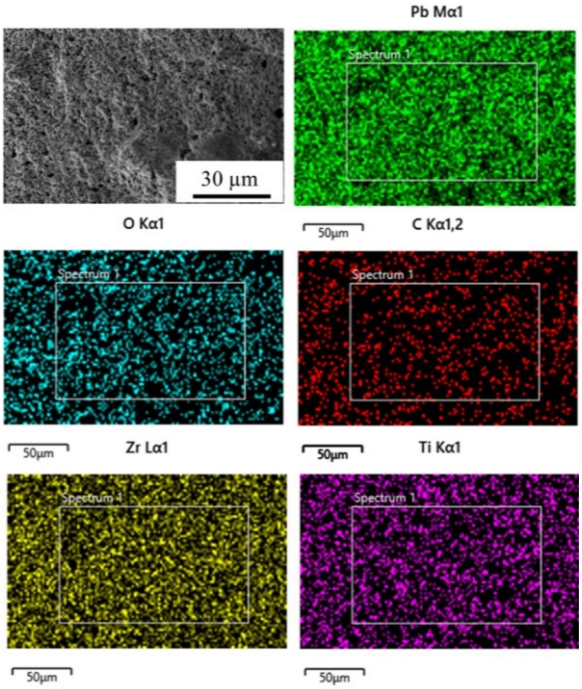

Fig. 8. Elemental analysis of the fiber extruded from paste 1.

Fig. 10 (a-b) presents a comparative SEM images of green and sintered PZT fibers. A noticeable reduction in fiber diameter is observed after sintering at 1250 °C, resulting from densification and shrinkage. This dimensional change is typical of ceramic sintering and confirms that the selected temperature produces structurally stable, crack-free fibers with improved packing density.

The SEM micrograph in Fig. 10(c) reveals the optimized microstructure of PZT fibers sintered at 1250 °C for 2 hours, highlighting the critical influence of paste viscosity control on final ceramic properties. The microstructure consists of well-defined, cuboid grains with a narrow size distribution, indicating controlled grain growth. Clean grain boundaries and the absence of secondary phases or microcracks confirm the effectiveness of the binder-plasticizer system in preventing defects. EDS analysis (Fig. 10(d)) confirmed the presence of titanium, zirconium, and lead oxides within the microstructure.

Surface porosity of the raw and sintered fibers was quantitatively evaluated using SEM micrographs analyzed

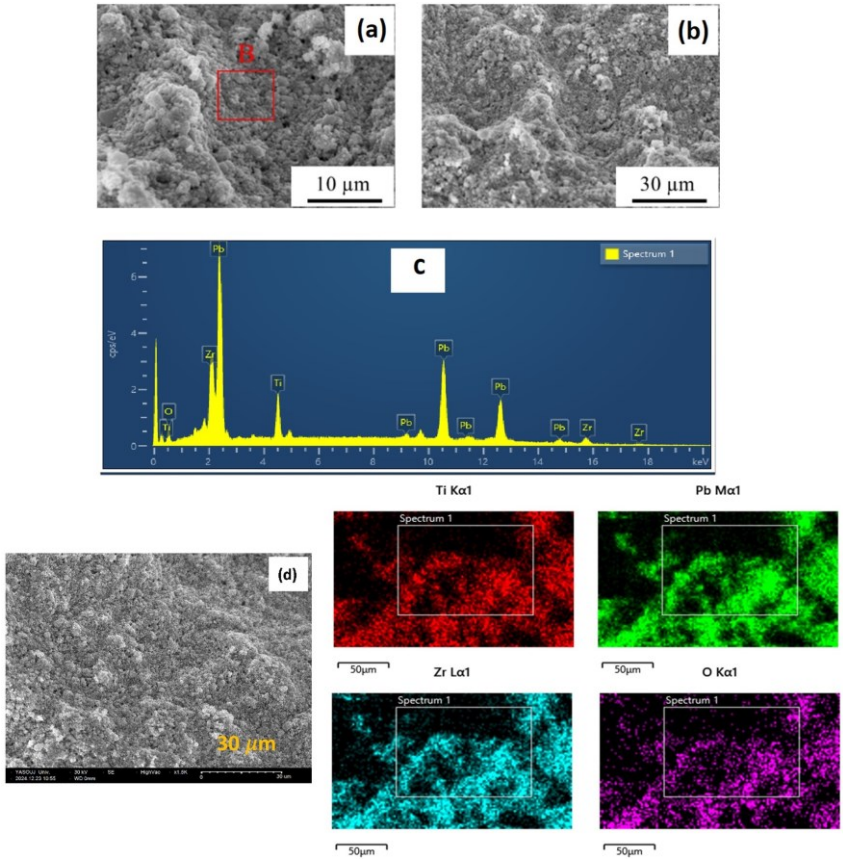

Fig. 9. (a, b) SEM micrographs, (c) EDS spectrum and (d) Elemental mapping of the fiber surface extruded from the optimal paste (sample 1) with increased DBF content (2.5 wt.%).

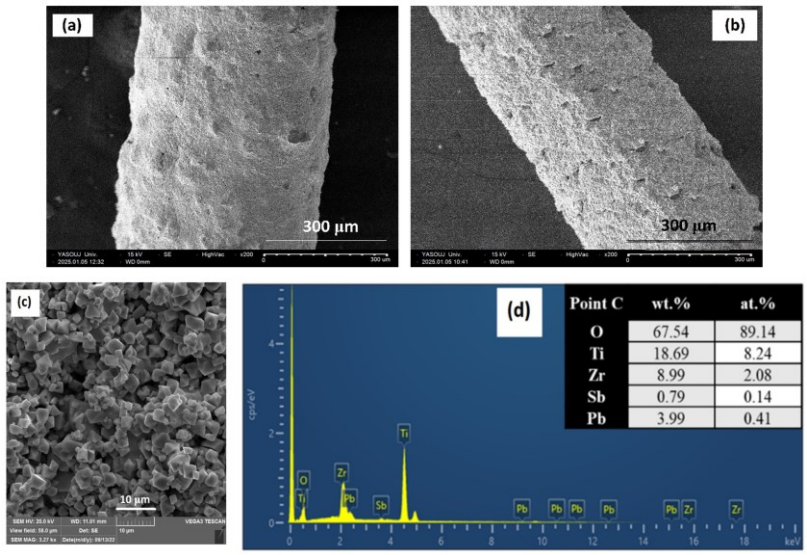

Fig. 10. SEM images of (a) the raw fiber's surface and (b) the surface of the fiber sintered at 1250 °C for 2 h, (c) the corresponding fracture surface, (d) the EDS analysis of the sample surface in (b).

via ImageJ, as shown in Fig. 11. The raw fibers (Fig. 11(a)) exhibited relatively high porosity of approximately 25%, indicating a loosely packed structure. In contrast, the sintered fibers (Fig. 11(b)) displayed significantly reduced porosity of about 5.5%, reflecting the densification during sintering. Archimedes-based density measurements revealed that the bulk density of the raw fibers was 4.72 g/cm³, (62% of the theoretical density). After sintering, the density increased to 7.19 g/cm³, reaching 94.4% of the theoretical density. This substantial densification, along with the reduction in surface porosity from 25% to 5.5%, confirms the improved structural compactness and mechanical integrity of the final PZT product.

For further analysis, Fig. 12 presents the elemental distribution on the surface of the sintered sample. Titanium (Ti), zirconium (Zr), oxygen (O), lead (Pb), and antimony (Sb) are uniformly distributed throughout the microstructure. This homogeneous distribution confirms the successful formation of the perovskite PZT phase and indicates that the solid-state reaction during sintering was complete, without compositional segregation that could compromise degrade piezoelectric performance.

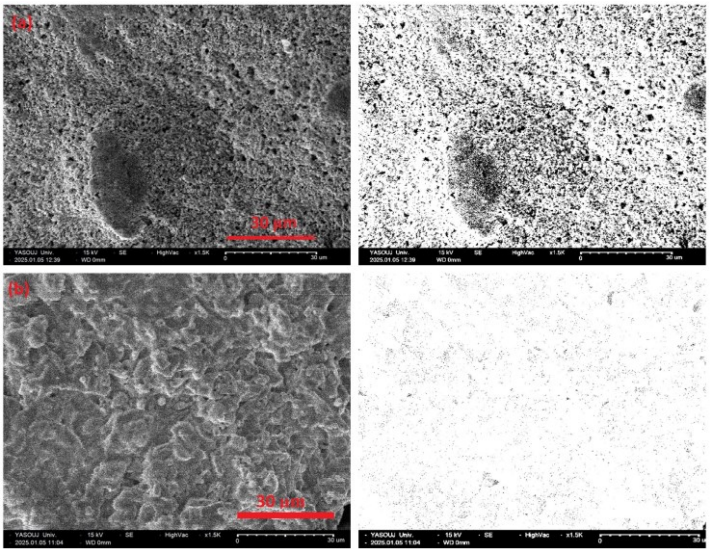

Fig. 11. SEM micrographs of (a) raw fiber and (b) sintered fiber (1250 ˚C, 2 h), along with the corresponding binary images processed using ImageJ for surface porosity analysis. The estimated porosity is ~25% for the raw fiber and ~5.5% for the sintered fiber.

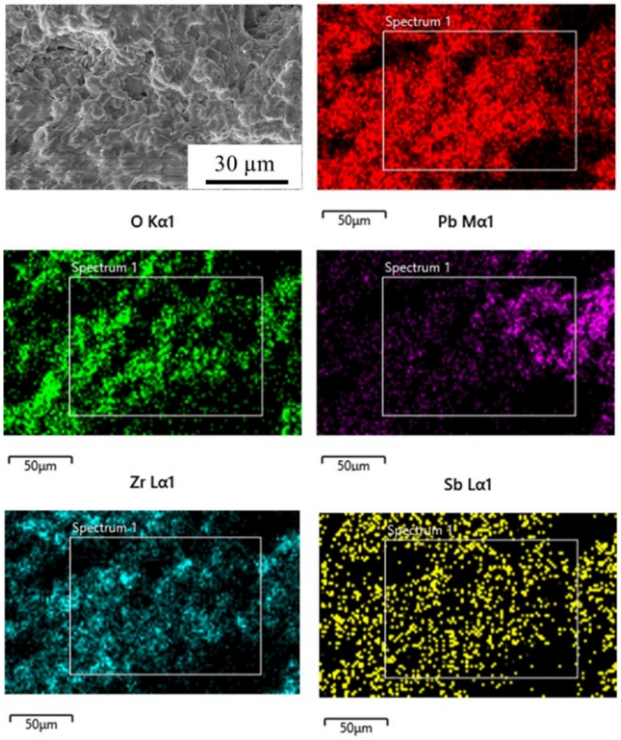

Fig. 12. mapping of the PZT fiber surface after sintering at 1250 ˚C for 2 hours.

4. Conclusions

This study investigated the fabrication and characterization of PZT fibers using an extrusion-based method. PZT pastes were systematically prepared with varying amounts of PVB, DBF, and SA additives, guided by a Taguchi experimental design. The formulation containing 5 wt.% PVB, 0.5 wt.% DBF, 0.8 wt.% SA, and 70 wt.% solid loading exhibited the most favorable rheological behavior, with a final viscosity of 15548 mPa·s, consistent with predictions from the Taguchi S/N analysis.

Subsequent adjustment of DBF content to 2.5 wt.% reduced the extrusion force required resulting in fibers with a more homogeneous microstructure and markedly lower porosity. The optimized paste was sintered at 1250 °C for 2 hours, yielding dense, uniform PZT fibers with well-developed grain structures. Surface porosity decreased from approximately 25% in the green fibers to ~5.5% after sintering, confirming effective densification and enhanced structural integrity.

Compared to previous studies that primarily focused on synthesis routes or post-processing properties, this work introduces a systematic, multiple additives formulation strategy coupled with rheological modeling. The integration of Taguchi design enabled precise optimization of paste composition, ensuring defect-free extrusion and dense, uniform sintered fibers. This methodology provides a framework for controlling viscosity and microstructure, representing a significant advancement in the extrusion processing of ceramic fibers.

Acknowledgement

The authors gratefully acknowledge the Central Laboratory of Yasouj University for providing the essential facilities and equipment that supported the successful completion of this research.

Authors' contributions

S. Abedini Nia: Measurements, Visualization, Writing-original draft

A. Shojaei Seyfabad: Data curation, Methodology

R. Hayati: Conceptualization, Resources, Supervision, Reviewing & Editing

Conflict of interest

There are no conflicts of interest.

Funding

The corresponding author would like to acknowledge the Deputy of research of Yasouj University for their financial support.

Data availability

The data is available on a reasonable request.

5. References

[1] Vaiani, L., Boccaccio, A., Uva, A. E., Palumbo, G., Piccininni, A., Guglielmi, P., Cantore, S., Santacroce, L., Charitos, I. A., Ballini, A. (2023). Ceramic materials for biomedical applications: An overview on properties and fabrication processes. *Journal of Functional Biomaterials, 14*(3), 146. https://doi.org/10.3390/jfb14030146

[2] Otitoju, T. A., Okoye, P. U., Chen, G., Li, Y., Okoye, M. O., & Li, S. (2020). Advanced ceramic components: Materials, fabrication, and applications. *Journal of*

Industrial and Engineering Chemistry, *85*, 34–65. https://doi.org/10.1016/j.jiec.2020.02.002

[3] Li, Z., Thong, H. C., Zhang, Y. F., Xu, Z., Zhou, Z., Liu, Y. X., Cheng, Y. Y., Wang, S.H., Zhao, C., Chen, F., & Bi, K. (2021). Defect engineering in lead zirconate titanate ferroelectric ceramic for enhanced electromechanical transducer efficiency. *Advanced Functional Materials*, *31*(15), 2005012. https://doi.org/10.1002/adfm.202005012

[4] Rao, R. G. S., & Kanagathara, N. (2015). Lead zirconate titanate: A piezoelectric material. *Journal of Chemical and Pharmaceutical Research, 7*(5), 921–923. https://doi.org/10.1016/J.NANOEN.2012.09.001

[5] Pan, D. (2024). Lead zirconate titanate (PZT) piezoelectric ceramics: Applications and prospects in human motion monitoring. *Ceramics-Silikáty, 68*(3), 444–458. https://doi.org/10.13168/cs.2024.0044

[6] Qiu, J., Tani, J., Yanada, N., Kobayashi, Y., & Takahashi, H. (2004). Fabrication of Pb(Nb,Ni)O_3–Pb(Zr,Ti)O_3 piezoelectric ceramic fibers by extrusion of a sol-powder mixture. *Journal of Intelligent Material Systems and Structures, 15*(9–10), 643–653. https://doi.org/10.1177/1045389x04043949

[7] Heiber, J., Clemens, F. J., Graule, T., & Hülsenberg, D. (2006). Influence of fibre diameter on the microstructure and the piezoelectric properties of PZT-fibres. *Advances in Science and Technology*, *45*, 2459–2463. https://doi.org/10.4028/www.scientific.net/AST.45.2459

[8] Guan, X., Chen, H., Xia, H., Fu, Y., Yao, J., & Ni, Q. Q. (2020). Flexible energy harvester based on aligned PZT/SMPU nanofibers and shape memory effect for curved sensors. *Composites Part B: Engineering, 197*, 108169. https://doi.org/10.1016/j.compositesb.2020.108169

[9] Guillot, F. M., Beckham, H. W., & Leisen, J. (2013). Hollow piezoelectric ceramic fibers for energy harvesting fabrics. *Journal of Engineered Fibers and Fabrics*, *8*(1), 155892501300800109. https://doi.org/10.1177/155892501300800109

[10] Meyer, R. J., Yoshikawa, S., & Shrout, T. R. (1996). Sol-gel-derived PZT fibers: Development and limitations. In *Smart Structures and Materials 1996: Smart Materials Technologies and Biomimetics* (*Vol. 2716*, pp. 69–79). SPIE. https://doi.org/10.1117/12.232126

[11] Yoshikawa, S., Selvaraj, U., Moses, P., Withams, J., Meyer, R., & Shrout, T. (1995). Pb(Zr,Ti)O_3 [PZT] fibers—Fabrication and measurement methods. *Journal of Intelligent Material Systems and Structures*, *6*(2), 152–158. https://doi.org/10.1177/1045389X9500600202

[12] Ismael, M. R., Clemens, F., Wyss, P., Graule, T., & Hoffmann, M. J. (2012). Processing and properties of co-extruded lead zirconate titanate fibers. *Journal of the American Ceramic Society*, *95*(1), 108–116. https://doi.org/10.1111/j.1551-2916.2011.04851.x

[13] Strock, H. B., Pascucci, M. R., Parish, M. V., Bent, A. A., & Shrout, T. R. (1999). Active PZT fibers: A commercial production process. In *Smart Structures and Materials 1999: Smart Materials Technologies* (*Vol. 3675*, pp. 22–31). SPIE. https://doi.org/10.1117/12.352799

[14] Ebru, M. A., Dagdeviren, C., & Papila, M. (2009). Pb(Zr,Ti)O_3 nanofibers produced by electrospinning process. *MRS Online Proceedings Library*, *1129*, 708. https://doi.org/10.1557/PROC-1129-V07-08

[15] Heiber, J., Clemens, F., Graule, T., & Hülsenberg, D. (2006). Influence of fibre diameter on the microstructure and the piezoelectric properties of PZT-fibres. *Advances in Science and Technology*, *45*, 2459–2463. https://doi.org/10.4028/www.scientific.net/AST.45.2459

[16] Qiu, J., Tani, J., Kobayashi, Y., Um, T. Y., & Takahashi, H. (2003). Fabrication of piezoelectric ceramic fibers by extrusion of Pb(Zr,Ti)O_3 powder and Pb(Zr,Ti)O_3 sol mixture. *Smart Materials and Structures*, 12(3), 331–337. https://doi.org/10.1088/0964-1726/12/3/303

[17] Mensur Alkoy, E., Dagdeviren, C., & Papila, M. (2009). Processing conditions and aging effect on the morphology of PZT electrospun nanofibers, and dielectric properties of the resulting 3–3 PZT/polymer composite. *Journal of the American Ceramic Society*, *92*(11), 2566-2570. https://doi.org/10.1111/j.1551-2916.2009.03261.x

[18] Yi, C. H., Lin, C.-H., Wang, Y. H., Cheng, S. Y., & Chang, H. Y. (2012). Fabrication and characterization of flexible PZT fiber and composite. *Ferroelectrics*, *434*(1), 91–99. https://doi.org/10.1080/00150193.2012.732513

[19] Hayati, R., Fereydoonpoor, I., & Fadaei, R. (2023). Investigating the effects of sintering variables on microstructure and density of PZT fibers fabricated via extrusion process. *Advanced Materials & Technologies*, *12*(2), 55–73. https://doi.org/10.30501/jamt.2023.411504.1287

[20] Cho, K. H., & Priya, S. (2011). Synthesis of ferroelectric PZT fibers using sol–gel technique. *Materials Letters*, *65*(4), 775–779. https://doi.org/10.1016/j.matlet.2010.11.070

[21] Heiber, J., Belloli, A., Ermanni, P., & Clemens, F. (2009). Ferroelectric characterization of single PZT fibers. *Journal of Intelligent Material Systems and Structures*, *20*(4), 379–385. https://doi.org/10.1177/1045389X08094365

[22] Rahsepar, H., Hayati, R., & Javadpour, S. (2024). Evaluation of the dielectric, and piezoelectric properties and optimizing the figure of merit of the 0–3 KNN-0.8ZnO/PVDF-HFP piezoelectric composite by the

Taguchi method. *Journal of Alloys and Compounds*, *1006*, 176373. https://doi.org/10.1016/j.jallcom.2024.176373

[23] Jia, X. (2023). The optimization of extrusion process parameters utilizing the Taguchi method. *International Journal of Frontiers in Engineering Technology*, *6*, 109–114. https://doi.org/10.25236/IJFET.2024.060418

[24] Chen, D. C., Chen, D. F., & Huang, S. M. (2024). Applying the Taguchi method to improve key parameters of extrusion vacuum-forming quality. *Polymers*, *16*(8), 1113. https://doi.org/10.3390/polym16081113

[25] Kozielski, L., Clemens, F., Lusiola, T., & Pilch, M. (2016). Uniaxial extrusion as an enhancement method of piezoelectric properties of ceramic micro fibers. *Journal of Alloys and Compounds*, *687*, 604–610. https://doi.org/10.1016/j.jallcom.2016.06.050

[26] Kumar, D., & Kumar, S. (2015). Process parameters optimization for HDPE material in extrusion blown film machinery using Taguchi method. *IOSR Journal of Mechanical and Civil Engineering*, 12(4), 1–3. https://doi.org/10.9790/1684-12450103

[27] Athreya, S., & Venkatesh, Y. (2012). Application of Taguchi method for optimization of process parameters in improving the surface roughness of lathe facing operation. *International Refereed Journal of Engineering and Science*, *1*(3), 13–19.

[28] Box, G. E. P. (1988). Signal-to-noise ratios, performance criteria, and transformations. *Technometrics*, *30*(1), 1–17. https://doi.org/10.2307/1270311

[29] Rathi, M. G., & Jakhade, N. A. (2014). An optimization of forging process parameter by using Taguchi method: An industrial case study. *International Journal of Scientific and Research Publications*, 4(6), 590–596.

[30] Janusas, G., Guobiene, A., Palevicius, A., Brunius, A., Cekas, E., Baltrusaitis, V., & Sakalys, R. (2017). Influence of binding material of PZT coating on microresonator's electrical and mechanical properties. In *Smart Sensors, Actuators, and MEMS VIII* (*Vol. 10246*, pp. 342–348). SPIE. https://doi.org/10.1117/12.2265978

[31] Wu, D., Qin, S., Liu, C.-L., Fang, B.-J., Cao, Z., & Cheng, J.-F. (2019). Surface modification by stearic acid on property of PLZT piezoelectric ceramics prepared via powder injection molding. *Journal of Inorganic Materials*, *34*(5), 535–540. http://doi.org/10.15541/jim20180323

[32] Jarray, A., Gerbaud, V., & Hemati, M. (2016). Stearic acid crystals stabilization in aqueous polymeric dispersions. *Chemical Engineering Research and Design*, *110*, 220–232. https://doi.org/10.1016/j.cherd.2016.02.028

[33] Nie, J., Li, M., Liu, W., Li, W., & Xing, Z. (2021). The role of plasticizer in optimizing the rheological behavior of ceramic pastes intended for stereolithography-based additive manufacturing. *Journal of the European Ceramic Society*, *41*(1), 646–654. https://doi.org/10.1016/j.jeurceramsoc.2020.08.013

[34] Rasteiro, M., & Salgueiros, I. (2005). Rheology of particulate suspensions in ceramic industry. *Particulate Science and Technology*, *23*(2), 145–157. https://doi.org/10.1080/02726350590922206

[35] De La Rosa, Á., Ruiz, G., Castillo, E., & Moreno, R. (2021). Calculation of dynamic viscosity in concentrated cementitious suspensions: Probabilistic approximation and Bayesian analysis. *Materials*, *14*(8), 1971. https://doi.org/10.3390/ma14081971

[36] Youness, D., Yahia, A., & Tagnit-Hamou, A. (2022). Development of viscosity models of concentrated suspensions: Contribution of particle-size and shape indices. *Construction and Building Materials*, *346*, 128335. https://doi.org/10.1016/j.conbuildmat.2022.128335

[37] Yue, Y., Ren, J., Yang, K., Wang, D., Qian, J., & Bai, Y. (2022). Investigation and optimisation of the rheological properties of magnesium potassium phosphate cement with response surface methodology. *Materials*, *15*(19), 6815. https://doi.org/10.3390/ma15196815

[38] Dulina, I., Umerova, S., & Ragulya, A. (2015). Plasticizer effect on rheological behaviour of screen printing pastes based on barium titanate nanopowder. *Journal of Physics: Conference Series*, *602*, 012035. https://doi.org/10.1088/1742-6596/602/1/012035

[39] Halbleib, L. L., Yang, P., Mondy, L. A., & Burns, G. R. (2005). The effects of process parameters on injection-molded PZT ceramics part fabrication—Compounding process rheology. *Sandia National Laboratories Technical Report*, SAND2005-2864. https://doi.org/10.2172/923077

[40] Waxman, R., Erturun, U., & Mossi, K. (2010). Feasibility of using piezoelectric probes to measure viscosity in Newtonian fluids. In *Smart Materials, Adaptive Structures and Intelligent Systems* (pp. 47–52). ASME. https://doi.org/10.1115/SMASIS2010-3688

[41] Restasari, A., Abdillah, L. H., Ardianingsih, R., Sitompul, H. R. D., Budi, R. S., Hartaya, K., & Wibowo, H. B. (2021). Thixotropic behavior in defining particle packing density of highly filled AP/HTPB-based propellant. *Symmetry*, *13*(10), 1767. https://doi.org/10.3390/sym13101767

[42] Powell, J., Assabumrungrat, S., & Blackburn, S. (2013). Design of ceramic paste formulations for co-extrusion. *Powder Technology*, *245*, 21–27. https://doi.org/10.1016/j.powtec.2013.04.017

[43] Bowen, C. R., Stevens, R., Nelson, L. J., Dent, A. C., Dolman, G., Su, B., Button, T. W., Cain, M. G., & Stewart, M. (2006). Manufacture and characterization of high activity piezoelectric fibres. *Smart Materials and*

Structures, *15*(2), 295–301. https://doi.org/10.1088/0964-1726/15/2/008

[44] Heiber, J., Clemens, F. J., Graule, T., & Hülsenberg, D. (2008). Influence of varying the powder loading content on the homogeneity and properties of extruded PZT-fibers. *Key Engineering Materials*, *368*, 11–14. https://doi.org/10.4028/www.scientific.net/KEM.368-372.11

[45] Rashid, T. N. I. T. A., Ahmad, Z. A., & Mohamad, H. (2021). Influence of sintering parameters on structural, dielectric and piezoelectric properties of Ca, La and Sr-doped PZT (PCLSZT) electroceramics. *Journal of Materials Science: Materials in Electronics*, *32*, 18095–18107. https://doi.org/10.1007/s10854-021-06354-y